Published in final edited form as:
Mol Pharm. 2013 October 7; 10(10): . doi:10.1021/mp4003688.

LHRH-targeted nanogels as delivery system for cisplatin to ovarian cancer

Natalia V. Nukolova[a,b,d], **Hardeep S. Oberoi**[c], **Yi Zhao**[c], **Vladimir P. Chekhonin**[b,d], **Alexander V. Kabanov**[a,c,*,§], and **Tatiana K. Bronich**[c,*]

[a] Department of Chemistry, Lomonosov Moscow State University, Leninskie Gory, Moscow, 119992, Russia.

[b] Department of Fundamental and Applied Neurobiology, Serbsky National Research Center for Social and Forensic Psychiatry, Kropotkinskiy 23, Moscow, 119991, Russia

[c] Department of Pharmaceutical Sciences and Center for Drug Delivery and Nanomedicine, College of Pharmacy, University of Nebraska Medical Center, 985830 Nebraska Medical Center, Omaha, NE 68198-5830, USA

[d] Russian State Medical University, Department of Medical Nanobiotechnology, Ostrovityanova 1, Moscow, 117997, Russia

Abstract

Targeted drug delivery using multifunctional polymeric nanocarriers is a modern approach for cancer therapy. Our purpose was to prepare targeted nanogels for selective delivery of chemotherapeutic agent cisplatin to luteinizing hormone-releasing hormone (LHRH) receptor overexpressing tumor *in vivo*. Building blocks of such delivery systems consisted of innovative soft block copolymer nanogels with ionic cores serving as a reservoir for cisplatin (loading 35%) and a synthetic analog of LHRH conjugated to the nanogels via poly(ethylene glycol) spacer. Covalent attachment of (D-Lys6)-LHRH to nanogels was shown to be possible without loss in either the ligand binding affinity or the nanogel drug incorporation ability. LHRH-nanogel accumulation was specific to the LHRH-receptor positive A2780 ovarian cancer cells and not towards LHRH-receptor negative SKOV-3 cells. The LHRH-nanogel cisplatin formulation was more effective and less toxic than equimolar doses of free cisplatin or untargeted nanogels in the treatment of receptor-positive ovarian cancer xenografts in mice. Collectively, the study indicates that LHRH mediated nanogel-cisplatin delivery is a promising formulation strategy for therapy of tumors that express the LHRH receptor.

Keywords

Nanogels; cisplatin; LHRH-targeting; targeted drug delivery; ovarian cancer

[*] Correspondence should be addressed to AVK and TKB Tel: (919) 537-3800; kabanov@email.unc.edu Tel: (402) 559-9351; Fax: (402) 559-9365; tbronich@unmc.edu.

[§]Current address: Center for Nanotechnology in Drug Delivery and Division of Molecular Therapeutics, UNC Eshelman School of Pharmacy, University of North Carolina at Chapel Hill, Genetic Medicine Building, room 1094, Campus Box 7362, Chapel Hill, NC 27599-7362

Supporting information

Additional figures depicting cellular uptake of nanogel in A2780 cells and tumor growth inhibition of ovarian xenografts in nude mice treated with CDDP formulations as well as UV spectra, ^{1}H-NMR spectra and MALDI-TOF mass spectra of LHRH and derivatives. This material is available free of charge via the Internet at http://pubs.acs.org.

1. Introduction

Chemotherapy continues to be a mainstay in treatment of a broad spectrum of malignancies, unfortunately with broad range of adverse side effects and limitations related to the intrinsic toxicity of the drugs to the normal tissues. Carrier-based drug delivery systems (polymer conjugates, liposomes, micelles, dendrimers, nanogels, inorganic or other solid particles, and others) are widely being investigated to overcome these limitations of conventional drug chemotherapy and improve its overall safety and patient convenience.[1, 2] Numerous preclinical and clinical studies employing such delivery systems have demonstrated an improved therapeutic effect and reduced overall toxicity, attributed primarily to the controlled drug release profile, altered drug pharmacokinetics and the enhanced permeability and retention (EPR) - mediated tumor accumulation of these carriers.[3-5] While the EPR guided strategy is passive in nature,[6] the development of next generation carriers with active targeting ligands associated with the carrier offers an opportunity to achieve a further improvement in therapeutic performance.[2, 7]

Receptors that are expressed primarily on cancer cells represent attractive molecular targets for selective drug delivery by this approach.[8] Luteinizing hormone-releasing hormone (LHRH, also known as gonadotropin-releasing hormone, GnRH) is a hormonal decapeptide and one such promising ligand.[9] It targets specific LHRH membrane receptors, which are characteristically overexpressed in many tumors including that of ovarian and endometrial (about 80%), prostate (about 90%), breast (about 50%), while its expression is scarce in healthy tissues.[10] Several studies have reported targeting the LHRH-receptor positive neoplasm utilizing agonistic and antagonistic analogs of LHRH peptide.[11-13] Studies employing LHRH-receptor targeted dendrimers,[14] nanoparticles,[15] liposomes,[16] etc. were able to substantially enhance intratumoral accumulation and anticancer efficacy, and hence indicates that LHRH-receptor mediated targeting is independent of the nanocarrier architecture, composition, size and molecular mass.[16]

Most of these studies have however focused on delivery of hydrophobic anticancer drugs (paclitaxel, methotrexate, camptothecin etc.), and have largely overlooked the more commonly used platinum anticancer complexes, which owing to their relative hydrophilicity provide substantial challenges to formulation in colloidal carriers. A recent class of high-capacity platinum-drug carriers based on block ionomer templates developed in our group overcomes many such limitations.[17] Capable of environmentally responsive swelling, these nanoscale ionic gels can incorporate platinum complexes at capacities exceeding 30 wt. %.[18-20] This is significantly higher than what has been reported for liposomes and other colloidal carriers.[5] Furthermore, the template assisted synthesis of nanogels by polyion complexation allows to produce the core-shell nanoparticles with controlled attachment of targeting ligands.[19] The purpose of this study was to expand the functionality of cisplatin-nanogels utilizing the specificity of LHRH mediated cellular targeting. For the first time we have shown LHRH-targeted cisplatin delivery and its enhanced anti-tumor effect *in vivo* using soft polyelectrolyte nanogels. Herein, we evaluate the drug therapeutic efficacy of LHRH-nanogels in an animal model of ovarian cancer.

2. Materials and methods

2.1. Materials

Poly(ethylene glycol)$_{170}$-*b*-poly(methacrylic acid)$_{180}$ (PEG-*b*-PMA) diblock copolymer (Mw/Mn=1.45) was from Polymer Source Inc. (Montreal, QC, Canada). (D-Lys6)-LHRH (Glp–His–Trp–Ser–Tyr–DLys–Leu–Arg–Pro–Gly) was from American Peptide Company (Sunnyvale, CA). Bifunctional Fmoc-NH-PEG-NHS and monofunctional methoxy-PEG-NH_2 with Mw (PEG)=10 kDa were from Creative PEGWorks (Winston Salem, NC). Micro

BCA protein colorimetric assay kit and Zeba spin desalting columns were from Thermo Fisher Scientific (Rockford, IL). Cisplatin (CDDP) and Pt standard for ICP-MS calibration were from Acros Organics (Geel, Belgium). CDDP for injection (Platinol®) was from Bristol Laboratories (Princeton, NJ). Iridium chloride internal standard for ICP-MS was from Spex Certiprep (Metuchen, NJ). Double distilled nitric acid 70% and hydrochloric acid 6 M were from GFS chemicals (Columbus, OH). Bio-safe Coomassie Blue G-250, Precision Plus Protein standards and Precast Gel for polyacrylamide electrophoresis (4-20% Tris-HCl) were from Bio-Rad Laboratories (Hercules, CA). Dimethylformamide (DMF), piperidine, tetraethylammonium chloride (TEA), 1,2-ethylenediamine (ED), 1-(3-dimethylaminopropyl)-3-ethylcarbodiimide hydrochloride (EDC), α-D-glucose (dextrose), ethylenediaminetetraacetic acid (EDTA), fluorescein isothiocyanate (FITC), 3-(4,5-dimethylthiazol-2-yl)-2,5-diphenyltetrazolium bromide (MTT), and other chemicals were from Sigma-Aldrich (St Louis, MO) and used as received.

2.2. Synthesis of LHRH-modified nanogels

The (D-Lys6)-LHRH was first reacted with NHS–PEG–Fmoc (molar ratio 1-1) in DMF in the presence of N,N-diisopropylethylamine (DIEA) for 2 h at room temperature (r.t.). Fmoc group was then removed using 30% piperidine/DMF for 45 min at r.t., followed by evaporation of organic solvents, and dialysis against phosphate buffered saline, PBS (overnight, 4°C, MWCO 3.5 kDa). The purified LHRH-PEG-NH_2 was lyophilized and stored at 4°C until further use.

PEG-*b*-PMA nanogels were prepared as described earlier [17] using block ionomer complex PEG-*b*-PMA/Ca^{2+} at a molar ratio of [Ca^{2+}]/[COO^-] = 1.3 with further cross-linking by ED and EDC ([EDC]/[ED] = 2; [COOH]/[EDC] = 5) at r.t., overnight. After through dialysis, 1% of carboxylic groups of nanogels (concentration of carboxylic groups was determined by potentiometric titration, 1 eq) were activated by excess of NHS/EDC (3 eq/2 eq). Then LHRH-PEG-NH_2 (1 eq) was added to the activated nanogel (PBS, pH 7.4) and stirred for 4 h at r.t. After that the LHRH-nanogel was purified using filtration on Amicon YM-30 filters (MWCO 30kDa, Millipore, Billerica, MA) at 3000 rpm for 10 min (4 washes). As a control methoxy-PEG-NH_2 (1 eq) was conjugated to nanogels in the same way.

To synthesize FITC-labeled nanogels, PEG-*b*-PMA chains were modified with FITC-ED,[19] titrated and then used for synthesis of the nanogels. The content of FITC in nanogels was determined by UV spectrometry at 490 nm in 50 mM bicarbonate buffer, pH 9.5.

2.3. Drug loading and release

Nanogel dispersion was mixed with CDDP (1 mg/ml) ([CDDP]/[COOH] = 0.5, pH 9.0, 37°C, 48 h). Unbound drug was removed by filtration on drug-pretreated Amicon YM-30 filters. Pt (Pt194/Pt195) was assayed on Nexion ion coupled plasma-mass spectrometer (NexION 300Q, PerkinElmer, Waltham, MA) calibrated with Pt (2-100 ng/ml). Samples were diluted in 0.1 N HCl. Drug loading capacity was calculated as percent ratio of mass of incorporated drug to total mass of drug-loaded nanogels without water.

Drug release was examined in PBS (pH 7.4, 0.14 M NaCl) and acetate buffered saline (ABS, pH 5.5, 0.14 M NaCl) at 37°C using Spectra/Por Float-A-Lyzer G2 dialysis systems (MWCO 3.5-5.0 kDa, Spectrum Labs, Rancho Dominguez, CA) and expressed as percent of total vs. time.

2.4. In vitro stability of nanogels

Targeted and untargeted nanogels were incubated in PBS or 20 vol % human plasma solution (prior centrifuged at 10000 g for 10 min to remove aggregates) at 37°C under gentle

stirring at concentration of 2 mg/ml. At each time point the particle size and polydispersity of nanoparticles were measured using dynamic laser light-scattering (DLS, Zetasizer Nano ZS, Malvern Instruments Ltd., MA) performed in triplicate at r.t.

2.5. Physicochemical characterization of LHRH-PEG-NH_2 and LHRH-nanogel

LHRH-PEG-NH_2 conjugates were analyzed by 1) proton nuclear magnetic resonance spectroscopy (^{1}H NMR) using Varian INOVA 500 NMR spectrometer (Varian, Palo Alto, CA) operating at 500 MHz (1 mg/ml, D_2O, pH 7.0, 25°C); 2) UV absorbance using SpectraMaxM5 spectrophotometer (Molecular Devices Co., Sunnyvale, CA), the UV spectra were recorded from 220 to 600 nm in PBS (0.5 mg polymer/ml); and 3) matrix-assisted laser desorption/ionization tandem time-of-flight (4800 MALDI-TOF/TOF, Applied Biosystems, Foster City, CA) mass spectrometry with a laser power of 3000 V, in positive reflector mode (10 mg/ml alpha cyano-4-hydroxycinnamic acid dissolved in 50% (v/v) aqueous acetonitrile containing 0.1% (v/v) TFA).

Nanoparticles were characterized by DLS for zeta (ζ)-potential, effective hydrodynamic diameters (D_{eff}), and polydispersity indexes (PdI), and by atomic force microscopy, AFM (average width (W_{av}) and height (H_{av})) as described previously [17]. The amount of LHRH conjugated to nanogels (μg protein per mg nanogel) was determined by micro BCA assay according to manufacturer's instructions.

Gel electrophoresis was performed using 4-20% Tris-HCl gel at 100 V for approximately 1 h in Mini-Protean Gel Electrophoresis System (Bio-Rad, Hercules, CA). Protein bands were visualized by staining with Bio-Safe Coomassie Blue G-250 Stain. PEG alone and LHRH-PEG samples were loaded at 30 μg PEG/well. Free LHRH, NHS-PEG-Fmoc and their mixture were used as controls.

2.6. Cell culture

A2780 human ovarian carcinoma cells were provided by Dr. P.Rogers (Institute of Cancer Research, University of Bristol, UK). SKOV-3 human ovarian carcinoma cells were provided by Dr. S.Batra (University of Nebraska Medical Center, Omaha, NE, USA). A2780 and SKOV-3 cells were cultured in the Gibco® RPMI 1640 or DMEM medium (Life Technologies, Grand Island, NY), respectively, supplemented with 2 mM glutamine, 10% (v/v) FBS, 100 U/ml penicillin and 0.1 mg/ml streptomycin at 37°C in a humidified atmosphere containing 5% CO_2. Cells were harvested with trypsin-EDTA (Life Technologies, Grand Island, NY) after 80% confluence.

2.7. Flow cytometry

Cells seeded at 50,000 cells per well in 24-well plates were grown in corresponding media for 2 days and then exposed to FITC-labeled nanogels (0-1 mg/ml) at 37°C for different times (0 to 3 h). After exposure they were washed three times with PBS, trypsinized at 37°C, centrifuged at 1500 rpm for 5 min and re-suspended in PBS (pH 7.4, 1% BSA). The % gated cells were analyzed using FACStarPlus flow cytometer operating under Lysis II program (Becton Dickinson, San Jose, CA) equipped with an argon ion laser.

2.8. Confocal microscopy

Cells (50,000 cells/chamber) were grown in Lab-Tek Chambered Cover Glass dishes in RPMI 1640 for 2 days and exposed to FITC-labeled nanogels (0.3 mg/ml) for 3 h at 37°C. After exposure cells were washed three times with PBS and kept in RPMI 1640 media prior to visualization by live cell confocal imaging (Carl Zeiss LSM 510, Carl Zeiss Inc., Thornwood, NJ).

2.9. Intracellular Pt accumulation

Cells were seeded in duplicate 25-cm^2 flasks, allowed to reach 80-90% confluence, and treated with free CDDP, nanogel/CDDP and LHRH-nanogel/CDDP for 24 h (37 °C) at CDDP equivalent concentrations of 0.5 mM. Following incubation, each flask was rinsed three times with PBS, trypsinized, aliquoted in duplicate at 1.5-ml microcentrifuge tubes and pelleted by centrifugation. One of each duplicate cell pellets was wet ashed by overnight incubation in 70% nitric acid at 60°C and analyzed for Pt content by ICP-MS. The other duplicate was lysed using M-PER mammalian protein extraction reagent (Thermo Scientific, Franklin, MA) and quantified for total protein using a micro BCA protein assay kit (Pierce, Rockford, IL). Whole cell uptake was expressed as ng Pt/mg cellular protein.

2.10. In vitro cytotoxicity

Cells seeded in 96-well plates (10,000 cells/well) 24 h before the experiment treated with 0-300 ug/ml CDDP, nanogels/CDDP and LHRH-CDDP for 24 h and then cultured for additional 48 h in drug-free media at 37°C. Cytotoxicity was determined by standard colorimetric MTT assay [21] and the IC_{50} values (dose that kills 50% cells) were calculated using GraphPad Prism Software.

2.11. In vivo antitumor activity

Four week old female athymic (nu/nu) mice (National Cancer Institute, Bethesda, MD) were housed in AAALAC accredited facility and quarantined for 7 days prior to tumor inoculation. Human ovarian tumor xengraft was initiated by injecting A2780 cells (5×10^6 cells/site) subcutaneously on the flanks, one above each hind limb. When tumor size was approximately 100-200 mm^3, animals were randomized based on tumor volume (4 groups, n=7-8). Treatments (5% dextrose, CDDP alone, nanogel/CDDP, LHRH-nanogel/CDDP) were administered via tail vein injections at 4-day intervals at CDDP equivalent dose of 4 mg CDDP/kg. The body weight and tumor volume were monitored every second day. Tumor volume, defined as $V = 0.5 \times L \times W^2$, was estimated by measuring two orthogonal diameters (longer dimension, L and smaller dimension, W) of the tumor using electronic calipers. Protocols were approved by the Institutional Animal Care and Use Committee. Animals were sacrificed when tumor volume exceeded 3000 mm^3, greatest tumor dimension exceeded 20 mm, tumor became necrotic, or animal exhibited a body weight loss of more than 20%. All other animals were sacrificed by day 23.

2.12. Detection of Pt accumulation in organs

For analysis of Pt profile the animals were euthanized on 20^{th} day of study and then perfused with about 30 ml saline. Liver, kidney, spleen and tumors were excised, washed with saline and frozen over dry ice before storage at −80°C. Known weights of thawed tissue were decomposed by wet ashing in screw cap vials with 6 volumes concentrated nitric acid, overnight heating and stirring at 60°C. Iridium internal standard was added prior to digestion. Platinum concentrations were read on Nexion ion coupled plasma-mass spectrometer (ICP-MS) calibrated with Pt (2-100 ng/ml) using iridium correction.

2.13. Statistics

In antitumor study, group means for tumor volume and body weights were evaluated using one way analysis of variance (ANOVA) followed by Tukey's test for group-wise comparisons. Survival was estimated using Kaplan-Meier analysis and compared using log-rank test (GraphPad Prism 5, GraphPad Software, Inc., La Jolla, CA). All other statistical comparisons were carried out using 2-tailed Student's t-test with unequal variance (Microsoft Excel 2007, Microsoft Corporation, WA). Differences were considered significant at $P < 0.05$.

3. Results

3.1. Preparation of cisplatin-loaded LHRH-nanogels

Polyelectrolyte PEG-*b*-PMA nanogel is a stable pH-responsive system for delivery of different chemotherapeutics.[20, 22, 23] Synthesis of cisplatin-loaded LHRH-targeted nanogels involved 1) conjugation of LHRH analog with heterobifunctional PEG linker, 2) preparation of drug loaded untargeted nanogels, and 3) attachment of PEGylated LHRH to the drug-loaded nanogels (**Figure 1**)

3.1.1. Synthesis and analysis of LHRH-PEG-NH_2 conjugate—Conjugation of LHRH peptide and Fmoc-PEG-NHS was carried out in DMF. First, in the presence of DIEA amine-reactive succinimidyl ester Fmoc-PEG-NHS was reacted with the lysine ε-amino group of LHRH, forming a stable amide bond. Then, Fmoc-deprotection by 30% piperidine/DMF was performed. All intermediates and final product were collected and analyzed using H^1-NMR and UV spectrometry. Alternatively, synthesis in aqueous media (PBS buffer) was attempted, but resulted in a small amount of white precipitates (**Figure S1**).

^{1}H-NMR spectrum of LHRH peptide with well-marked alpha and beta protons as well as aromatic protons (Trp, Tyr) was received (**Figure S2a**). In NHS-PEG-Fmoc spectrum the chemical shift at 3.61 ppm was typical for oxymethylene protons in PEG, shifts at 7.2–7.8 ppm and 5.3 ppm were corresponded to protective Fmoc group and signal at 2.8 ppm was attributed to NHS methylene in ^{1}H-NMR spectra (**Figure S2b**). In the spectra of LHRH-PEG-Fmoc, successful PEGylation was indicated by the appearance of signals corresponding to PEG (3.6 ppm) and Fmoc (7.2–7.8 ppm) as well as disappearance of chemical shift which belongs to NHS group (2.8 ppm) (**Figure S2c**). The deprotection was confirmed by disappearance of Fmoc signals in LHRH-PEG-NH_2 spectrum (**Figure 2a**).

Further, the LHRH-PEG conjugate was analyzed by gel electrophoresis. As shown in **Figure 2b** the PEG polymer migrated in the gel, and a faint intensity band was detected in lane 3. For LHRH-PEG conjugates (lanes 4 and 5), which had molecular weight similar to free PEG (11 kDa vs. 10 kDa), the high density bands appeared in the same region of the gel with no free LHRH detected. This indicates thorough purification and successful PEGylation of protein. To increase the efficiency of LHRH-PEG synthesis we attempted conjugation using an excess of NHS-PEG-Fmoc. However, such conditions led to formation of peptide modified with multiple PEG chains. For example, several additional bands (**Figure 2b** lane 4), corresponding to conjugates with multiple PEG chains, were observed when 5-fold molar excess of NHS-PEG-Fmoc was used. MALDI-TOF data also suggested that double modified peptide LHRH-$(PEG)_2$ could be formed during reaction with excess of NHS-PEG-Fmoc (5 eq.). Hence for subsequent studies 1 eq. NHS-PEG-Fmoc was used for the reaction which generated mono PEG substituted LHRH (**Figure S3**).

UV analysis of precursors, intermediates and final product detected a shift and decrease in UV absorbance at ~ 260 nm, indicating successful Fmoc-deprotection of PEG chain (**Figure 2c**). The presence of the peak at 270-280 nm in the final product indicates the peptide incorporation to PEG chain (**Figure S1**). Combination of these methods confirmed successful LHRH-PEG conjugation.

3.1.2. Synthesis and analysis of LHRH-nanogels—Soft polymeric nanogels were prepared by template-assisted method involving condensation of PEG-*b*-PMA by Ca^{2+} ions, followed by chemical cross-linking of the polyion chains in their cores. The resulting nanogels represented core-shell nanoparticles with pH-dependent swelling behavior.[18] The physicochemical characteristics of LHRH-nanogels were quite similar to untargeted nanogels (**Table 1**), and both negatively charged nanoparticles were characterized by narrow

size distribution. The morphology and size of nanogels were further analyzed by tapping-mode AFM in air. AFM studies suggested that nanogels had a spherical morphology (**Figure 2d**). The high aspect ratio, W_{av}/H_{av} denoted substantial flattening of the nanogel particles, which reflects their "softness".[17] Unmodified nanogels were more flat or "soft" than LHRH-nanogels. The measured H_{av} and W_{av} were also used to estimate the volumes of the nanogels in the dry state: 11228 and 10974 nm^3 for LHRH-nanogels and nanogels, respectively. LHRH-modified nanogels were also analyzed by ^{1}H-NMR (data not shown), however, the overlap between LHRH-PEG and nanogels (PMA-*b*-PEG) peaks prevented estimation of exact number of LHRH molecules per nanogel based on integration. LHRH-targeted nanogels contained 80-100 μg protein per mg of nanogel as assessed by BCA assay. Previously using folate-decorated nanogels we have shown that attachment of the targeting group should be carried out after nanogels loading with CDDP to avoid "poisoning" of the targeting by this drug.[19] In the present case the order of the drug loading and LHRH attachment does not seem to be that important as it did not affect cellular uptake of targeted nanogels discussed below.

3.1.3. Synthesis and analysis of CDDP-loaded nanogels—The maximum drug content in the nanogels could be achieved by incubation of CDDP with the aqueous dispersions of nanogels for 48 h at pH 9.0 [22]. Nanogels efficiently incorporated CDDP (loading capacity >35%, **Table 2**) and remained stable in PBS or plasma at 37 °C without aggregation for at least 15 days (**Figure 3b**). The net negative charge and particle size of nanogels decreased upon drug loading due to progressive neutralization and condensation of the PMA segments by CDDP (**Table 2**).

Both CDDP-loaded formulations displayed similar pH-dependent sustained release profile without burst release (**Figure 3a**), which indicates that the modification of nanogels with targeting groups had no influence on drug retention. The accelerated release at the acidic pH (ABS buffer) could be due to the protonation of carboxylic groups of PMA segments, which weakened the drug and nanogel electrostatic coupling and was discussed previously.[19]

3.2. Cellular uptake and cytotoxicity study

Human ovarian carcinomas A2780 and SKOV-3 cells known for their high and low levels of LHRH receptor expression, respectively,[24] were used for these studies (**Figure S4**). The cellular uptake of LHRH-nanogels greatly exceeded the uptake of untargeted nanogels in A2780 cells (**Figure 4a**). Notably, at 30 min the cellular uptake of untargeted nanogels was about 3%, while the uptake of LHRH-nanogels was 47%. On the other hand, only a marginal difference in accumulation of targeted and untargeted nanogels was observed with SKOV-3 cells (**Figure 4a** and **S6**). In any case the overall cellular accumulation in SKOV-3 cells was comparable to that of untargeted nanogels in A2780 cells (5-10%). The uptake of nanogels (with and without the LHRH-moiety) was concentration-dependent and to a lesser extent time-dependent (**Figure 4a** and **S5**). As expected, the difference in accumulation of targeted and untargeted nanogels in A2780 cells decreased with increasing of nanocarrier concentration. Thus, at low concentration (0.1 mg/ml, 3 h incubation) the cellular uptake of LHRH-targeted nanogel was more than 9 times higher than for untargeted nanogels, but at high concentration of polymer (1 mg/ml, 3 h) this difference was only 2 times (**Figure S5**). Enhanced uptake of targeted nanogels was confirmed by confocal study on A2780 cells (**Figure 4c**).

Furthermore, using ICP-MS we determined the total Pt accumulation in the cells after their treatment with drug-loaded nanogels (**Figure 4b**). To be able to obtain detectable amounts of Pt in the cells, A2780 and SKOV-3 cells were treated with high concentration of drug-loaded nanogels for 24 h. Since the uptake of nanogels was concentration and time-

dependent, no major difference in Pt accumulation between studied formulations was observed in these experiments (> 0.5 mg/ml, 24 h) in sharp contrast to what was detected by flow cytometry (0.1 mg/ml, 3 h). However, even under these conditions the LHRH-nanogels/CDDP showed higher accumulation of Pt in comparison with untargeted nanogels (about 1.6 times) in A2780 cells. In case of SKOV-3 cells this correlation was not observed. It should be noted that the accumulation of free drug exceeded that of CDDP-loaded nanogel in both cell lines (data not shown).

Next, we examined the cytotoxicity of the targeted and untargeted CDDP-loaded nanogels by MTT test. As expected, the cytotoxicity of CDDP was greatly decreased after its incorporation into the nanogels (by nearly 10-times in the case of untargeted nanogels for 24 h treatment). This was presumably due to slower entry of the CDDP-loaded nanogels into cells and slow release of the bound drug from the nanogels.[19, 22] The cytotoxicity of targeted CDDP-loaded nanogels was increased considerably compared to that of untargeted CDDP-loaded nanogels (IC_{50} CDDP equivalents in μg/ml: 9.24±0.9 vs. 16.33±1.3). Importantly, the unloaded nanogels alone did not exhibit a cytotoxic effect under these conditions. Taken together these data suggest that LHRH-targeted moiety provided not only enhanced accumulation of LHRH-nanogels in the receptor-positive cell line but also significantly increased cytotoxicity of drug-loaded targeted nanogels.

3.3. In vivo antitumor activity

We analyzed the antitumor activity of the different cisplatin formulations (CDDP alone, nanogel/CDDP, LHRH-nanogel/CDDP) using four-week old nude athymic (nu/nu) mice bearing xenografts of human ovarian tumor. All formulations were injected at equivalent dose of CDDP (4 mg/kg) [25] and displayed the suppression of tumor growth in comparison with control group dextrose (**Figure 5a**). Free CDDP and nanogel/CDDP had a similar impact on the tumor burden till the end of the treatment (12^{th} day), but thereafter the suppression of tumor growth in nanogel/CDDP group was better compared to free drug. On the contrary, LHRH-nanogel/CDDP significantly decreased the tumor volume compared to other groups during entire studied period ($P < 0.05$). In animals treated with LHRH-nanogel/CDDP the tumor inhibition (TI%) reached a maximum of about 75% on the second day of treatment and did not change significantly thereafter (20 days), **Figure S7**. In animals treated with free CDDP the values of TI% gradually increased reaching its maximum of about 50% only after a week. A similar situation was observed for nanogel/CDDP treated group (TI% of about 50% at fourth day). Also, animals treated with CDDP-loaded targeted nanogels had prolonged survival time compared with all other groups (**Figure 5c**). Moreover, no significant changes in body weight were observed for control and drug-loaded nanogel groups, indicating that all treatments were well tolerated (**Figure 5b**). In contrast, animals treated by free CDDP experienced a major lost in body weight after two weeks. Thus, at the doses and schedules of administration used in the present study CDDP loaded in nanogels had significantly lower systemic toxicity than free drug (**Figure 5b**).

Furthermore, we used ICP-MS to analyze the tumor and organ accumulation of Pt in animals treated with various CDDP formulations, sacrificed on 20^{th} day of the study (**Figure 5d)**. Consistent with our previous report [19] only a trace amount of Pt was detected for free CDDP in major organs (kidney, liver and spleen). In groups treated with drug-loaded nanogels the high level of Pt was recorded in the organs of reticuloendothelial system, such as spleen and liver. However no histopathological changes were observed in any nanogel treatment groups (**Figure S8**). Also, our data confirmed the targeted delivery of CDDP using LHRH-nanogels in A2780 human ovarian cancer model. Thus, even 20^{th} days after the initiation of the treatment the tumor accumulation of Pt in the group treated with LHRH-nanogel/CDDP was 23% higher than that in the group treated with non-targeted nanogel/CDDP and 80% higher

than that in the group which received CDDP alone (insert in **Figure 5d**). A more detailed analysis of biodistribution at the earlier time points would however be needed to confirm the specificity of the LHRH-targeting mechanism *in vivo.*

4. Discussion

Polyelectrolyte PEG-*b*-PMA nanogels are stable, negatively charged, spherical nanoparticles with narrow polydispersity (**Table 1**). Nanogels comprise nearly 95% water, and can serve as carriers for different types of hydrophilic drugs with remarkably high loading capacity (cisplatin, 35% w/w;[18, 19] doxorubicin 45% w/w [26]), where drug retention can be achieved by either covalent or non-covalent interactions. As discussed in our previous publication [19] the hydrodynamic size of nanogels depends upon the balance of the chain ionization, electrostatic repulsion and osmotic effect within the nanogels. Nanogels easily swell upon increasing pH [18] and the effects of pH on their size and ζ-potential are suppressed as the ionic strength increases (0.15 M buffered saline vs. distilled water), probably, due to the masking of the electrostatic charge by the electrolyte. At the same pH 7.4 the particle size and net negative charge of nanogels decreased when salt was added (**Table 1**), albeit a more complex behavior could be observed at different pH as discussed elsewhere.[19] To maximize drug loading in the nanogels the optimal choice of pH and ionic strength is important.[22] Specifically, based on our prior report we have chosen a relatively high pH 9.0 and salt free conditions for drug loading to 1) ensure deprotonation of carboxylate groups in nanogels, 2) maximize swelling of nanogel core and 3) prevent displacement of the drug by low molecular weight counterion, such as chloride, phosphate, carbonate, and acetate anions [27, 28] (**Table 2**).

Previously we reported the possibility of targeted delivery of CDDP-loaded nanogels through their surface modification by folic acid derivative towards folate receptor positive ovarian cancer cells.[19] However, we also observed an increased accumulation of Pt in the kidney due to relatively high expression of folate receptors in the kidney.[29] Although the increased kidney accumulation did not result in any visible toxicity, it still remains a concern taking into account that kidney is the main site of the platinum drug toxicity.[30] In the current study we selected an alternate targeting moiety with a better selectivity towards the tumor. Receptors for LHRH are known to be overexpressed in breast, ovarian and prostate cancer cells but lack any detectable expression in visceral organs.[10] Therein, nanogels were modified by a LHRH analog using the bifunctional PEG-linker for active delivery of CDDP to the LHRH-positive ovarian cancer *in vivo*. PEGylation of LHRH and its attachment to nanogel surface was successfully achieved and validated (**Figure 2**). A major concern with bioconjugation of peptide targeting ligands is a loss in their binding affinity due to modification of an essential residue. However, covalent attachment of even bulky molecules to ε-amino group of the lysine residue of (D-Lys6)-LHRH is possible without loss of its ability to bind to LHRH receptors and it is a commonly used approach for LHRH modifications.[10] Our data (**Figure 4**) corroborate that LHRH-targeting groups retained their activity and promoted accumulation of LHRH-nanogels in the LHRH-positive cells due to receptor endocytosis.

Attachment of LHRH to nanocarrier did not significantly affect their drug loading capacity and release profile (**Table 2**). Both formulations were capable of sustained drug release over long period of time with no burst (**Figure 3a**). Stability experiments showed that the synthesized drug-loaded LHRH-nanogels were stable in PBS or plasma at 37°C for 2 weeks (**Figure 3b**). Therefore the nanogels are expected to be stable and retain sufficient amounts of drug after systemic administration. Accelerated drug release is likely upon internalization of these nanogels in the tumor cells if this process involves routing to acidic intracellular compartment.

Uptake of LHRH-nanogels and intracellular accumulation of its cisplatin cargo were superior to that of untargeted nanogels in LHRH-receptor overexpressing A2780 cells (**Figure 4**), but not in LHRH-receptor negative SKOV-3 cells,[24] indicating the involvement of receptor mediated endocytosis. However, despite the enhanced cellular accumulation of LHRH-nanogels, the formulation had a diminished cytotoxicity compared to the free cisplatin *in vitro*. This is likely due to the slow release of the encapsulated drug from nanocarrier (**Figure 3**) and slower accumulation of nanogels in the cells in comparison with the free drug. Nonetheless, a cumulative effect of targeted delivery moiety and pH-dependent induced drug release at the target site was expected to translate into effective tumor growth reduction *in vivo*.

To evaluate the influence of LHRH-targeting group on the delivery of cisplatin to its targeted site we used mice bearing xenografts of A2780 human ovarian cancer. Tumor growth for different formulations exhibited the trend: control >> CDDP > nanogel/CDDP >> LHRH-nanogel/CDDP (**Figure 5a**). Tumor growth reduction in CDDP and nanogel/CDDP groups could be distinguished only at the end of the treatment (second week). This could be due to one or more the following reasons: 1) CDDP owing to its low molecular weight was rapidly removed by the renal system in contrast to CDDP-loaded nanogels that exceeded the renal clearance limit [1] and possibly remained longer in blood circulation, 2) the increased tumor accumulation of the drug-loaded nanogels was aided by passive targeting due to EPR-effect;[6] and 3) circulating nanogels could also serve as a depot for a sustained release of CDDP which resulted in the increased overall exposure of tumor to the drug (**Figure 3a** and **Figure 5d**). The LHRH-targeting groups further significantly improved the antitumor effect of the drug-loaded nanogels. The difference in the tumor inhibition (TI%) between free CDDP and LHRH-nanogel/CDDP was about 25-30% during entire period of observation. Preliminary results on biodistribution of Pt also indicated that LHRH-moiety contributes to the accumulation of the drug in the target site. Notably on day 20 after treatment initiation the Pt accumulation in tumor enhanced in LHRH-nanogels/CDDP group compared to other groups (**Figure 5d**). Both targeted and untargeted drug loaded nanogels displayed considerable accumulation of Pt in the highly perfused organs such as liver and spleen. This could be a result of combined activity of the circulating blood passing through the organs and uptake of nanogels by cells of reticuloendothelial system. It was not a surprise since it is known that these organs are responsible for elimination of various nanoparticles from the circulation.[2, 5] Nevertheless these data suggest that the targeted delivery of CDDP was more effective in comparison with passive targeting of CDDP-nanogel by the EPR phenomenon.

It should be noted, that numerous systemic toxicities such as nephrotoxicity and neurotoxicity prevent administration of higher cisplatin doses during therapy. Loading of CDDP into the nanocarriers could allow using higher drug doses. In support of this assumption **Figure 5b** shows that both targeted and untargeted drug loaded nanogels did not induce body weight loss while the same dose of the free CDDP produced a considerable body weight loss ($P < 0.05$), which indicated systemic toxicity of free CDDP. This data is consistent with other publications related to the detailed toxicity analysis of CDDP-loaded nanocarriers and confirmed that systemic toxicity associated with CDDP is more profound in case of free drug administration than for the drug-loaded formulations.[25, 31, 32] As a result, animals treated with CDDP-loaded targeted nanogels had prolonged survival time compared with all other groups (**Figure 5c**).

Therefore we demonstrated that the LHRH-nanogels/CDDP was more effective and less toxic than equimolar doses of free CDDP or nanogels/CDDP in the treatment of LHRH receptor-positive cancers in mice by active targeted delivery of CDDP to the tumor. Collectively, these data indicated that the LHRH-nanogels/CDDP could be used for the

targeted therapy of tumors that express LHRH receptors such as A2780 ovarian cancer. In addition to that, this drug delivery system might also find application in the treatment of breast and prostate cancers as they are known for LHRH overexpression.[10, 12]

Supplementary Material

Refer to Web version on PubMed Central for supplementary material.

Acknowledgments

This work was supported by the grants from U.S.A. National Institute of Health CA116590 (T.K.B.) and from Government of the Russian Federation Ministry of Science and Education grant 11.G34.31.0004 (A.V.K.). We thank UNMC Nuclear Magnetic Resonance Facility (Ed Ezell) for acquisition of NMR data and summer intern Jerome Prusa for his help with analysis of LHRH-nanogels. We acknowledge the assistance of the Nanomaterials Core facility of the Center for Biomedical Research Excellence (CoBRE) Nebraska Center for Nanomedicine supported by the NIH grant RR021937.

References

1. Duncan R. The dawning era of polymer therapeutics. Nat Rev Drug Discov. 2003; 2:347–60. [PubMed: 12750738]
2. Petros RA, DeSimone JM. Strategies in the design of nanoparticles for therapeutic applications. Nat Rev Drug Discov. 2010; 9:615–27. [PubMed: 20616808]
3. Vicent MJ, Duncan R. Polymer conjugates: nanosized medicines for treating cancer. Trends Biotechnol. 2006; 24:39–47. [PubMed: 16307811]
4. Moghimi SM, Hunter AC, Murray JC. Nanomedicine: current status and future prospects. FASEB J. 2005; 19:311–30. [PubMed: 15746175]
5. Torchilin VP. Multifunctional nanocarriers. Adv Drug Deliv Rev. 2006; 58:1532–55. [PubMed: 17092599]
6. Maeda H, Wu J, Sawa T, Matsumura Y, Hori K. Tumor vascular permeability and the EPR effect in macromolecular therapeutics: a review. J Control Release. 2000; 65:271–84. [PubMed: 10699287]
7. Davis ME, Chen ZG, Shin DM. Nanoparticle therapeutics: an emerging treatment modality for cancer. Nat Rev Drug Discov. 2008; 7:771–82. [PubMed: 18758474]
8. Mohanty C, Das M, Kanwar JR, Sahoo SK. Receptor mediated tumor targeting: an emerging approach for cancer therapy. Curr Drug Deliv. 2011; 8:45–58. [PubMed: 21034422]
9. Schally AV, Arimura A, Kastin AJ, Matsuo H, Baba Y, Redding TW, Nair RM, Debeljuk L, White WF. Gonadotropin-releasing hormone: one polypeptide regulates secretion of luteinizing and follicle-stimulating hormones. Science. 1971; 173:1036–8. [PubMed: 4938639]
10. Nagy A, Schally AV. Targeting of cytotoxic luteinizing hormone-releasing hormone analogs to breast, ovarian, endometrial, and prostate cancers. Biol Reprod. 2005; 73:851–9. [PubMed: 16033997]
11. Schally AV, Nagy A. Cancer chemotherapy based on targeting of cytotoxic peptide conjugates to their receptors on tumors. Eur J Endocrinol. 1999; 141:1–14. [PubMed: 10407215]
12. Dharap SS, Wang Y, Chandna P, Khandare JJ, Qiu B, Gunaseelan S, Sinko PJ, Stein S, Farmanfarmaian A, Minko T. Tumor-specific targeting of an anticancer drug delivery system by LHRH peptide. Proc Natl Acad Sci U S A. 2005; 102:12962–7. [PubMed: 16123131]
13. Sundaram S, Trivedi R, Durairaj C, Ramesh R, Ambati BK, Kompella UB. Targeted drug and gene delivery systems for lung cancer therapy. Clin Cancer Res. 2009; 15:7299–308. [PubMed: 19920099]
14. Minko T, Patil ML, Zhang M, Khandare JJ, Saad M, Chandna P, Taratula O. LHRH-targeted nanoparticles for cancer therapeutics. Methods Mol Biol. 2010; 624:281–94. [PubMed: 20217603]
15. Taheri A, Dinarvand R, Ahadi F, Khorramizadeh MR, Atyabi F. The in vivo antitumor activity of LHRH targeted methotrexate-human serum albumin nanoparticles in 4T1 tumor-bearing Balb/c mice. Int J Pharm. 2012; 431:183–9. [PubMed: 22531853]

16. Saad M, Garbuzenko OB, Ber E, Chandna P, Khandare JJ, Pozharov VP, Minko T. Receptor targeted polymers, dendrimers, liposomes: which nanocarrier is the most efficient for tumor-specific treatment and imaging? J Control Release. 2008; 130:107–14. [PubMed: 18582982]
17. Bronich TK, Keifer PA, Shlyakhtenko LS, Kabanov AV. Polymer micelle with cross-linked ionic core. J Am Chem Soc. 2005; 127:8236–7. [PubMed: 15941228]
18. Kim JO, Nukolova NV, Oberoi HS, Kabanov AV, Bronich TK. Block Ionomer Complex Micelles with Cross-Linked Cores for Drug Delivery. Polym Sci Ser A Chem Phys. 2009; 51:708–718.
19. Nukolova NV, Oberoi HS, Cohen SM, Kabanov AV, Bronich TK. Folate-decorated nanogels for targeted therapy of ovarian cancer. Biomaterials. 2011; 32:5417–26. [PubMed: 21536326]
20. Oberoi HS, Nukolova NV, Zhao Y, Cohen SM, Kabanov AV, Bronich TK. Preparation and In Vivo Evaluation of Dichloro(1,2-Diaminocyclohexane)platinum(II)-Loaded Core Cross-Linked Polymer Micelles. Chemother Res Pract. 2012; 2012:905796. [PubMed: 22844591]
21. Mosmann T. Rapid colorimetric assay for cellular growth and survival: application to proliferation and cytotoxicity assays. J Immunol Methods. 1983; 65:55–63. [PubMed: 6606682]
22. Oberoi HS, Laquer FC, Marky LA, Kabanov AV, Bronich TK. Core cross-linked block ionomer micelles as pH-responsive carriers for cis-diamminedichloroplatinum(II). J Control Release. 2011; 153:64–72. [PubMed: 21497174]
23. Chacko RT, Ventura J, Zhuang J, Thayumanavan S. Polymer nanogels: A versatile nanoscopic drug delivery platform. Adv Drug Deliv Rev. 2012; 64:836–851. [PubMed: 22342438]
24. Taratula O, Garbuzenko OB, Kirkpatrick P, Pandya I, Savla R, Pozharov VP, He H, Minko T. Surface-engineered targeted PPI dendrimer for efficient intracellular and intratumoral siRNA delivery. J Control Release. 2009; 140:284–93. [PubMed: 19567257]
25. Oberoi HS, Nukolova NV, Laquer FC, Poluektova LY, Huang J, Alnouti Y, Yokohira M, Arnold LL, Kabanov AV, Cohen SM, Bronich TK. Cisplatin-loaded core cross-linked micelles: comparative pharmacokinetics, antitumor activity, and toxicity in mice. Int J Nanomedicine. 2012; 7:2557–71. [PubMed: 22745537]
26. Kim JO, Kabanov AV, Bronich TK. Polymer micelles with cross-linked polyanion core for delivery of a cationic drug doxorubicin. J Control Release. 2009; 138:197–204. [PubMed: 19386272]
27. Todd RC, Lovejoy KS, Lippard SJ. Understanding the effect of carbonate ion on cisplatin binding to DNA. J Am Chem Soc. 2007; 129:6370–1. [PubMed: 17465550]
28. Segal E, Le Pecq JB. Role of ligand exchange processes in the reaction kinetics of the antitumor drug cis-diamminedichloroplatinum(II) with its targets. Cancer Res. 1985; 45:492–8. [PubMed: 4038470]
29. Low PS, Henne WA, Doorneweerd DD. Discovery and development of folic-acid-based receptor targeting for imaging and therapy of cancer and inflammatory diseases. Acc Chem Res. 2008; 41:120–9. [PubMed: 17655275]
30. Arany I, Safirstein RL. Cisplatin nephrotoxicity. Seminars in nephrology. 2003; 23:460–464. [PubMed: 13680535]
31. Uchino H, Matsumura Y, Negishi T, Koizumi F, Hayashi T, Honda T, Nishiyama N, Kataoka K, Naito S, Kakizoe T. Cisplatin-incorporating polymeric micelles (NC-6004) can reduce nephrotoxicity and neurotoxicity of cisplatin in rats. Br J Cancer. 2005; 93:678–87. [PubMed: 16222314]
32. Newman MS, Colbern GT, Working PK, Engbers C, Amantea MA. Comparative pharmacokinetics, tissue distribution, and therapeutic effectiveness of cisplatin encapsulated in long-circulating, pegylated liposomes (SPI-077) in tumor-bearing mice. Cancer Chemother Pharmacol. 1999; 43:1–7. [PubMed: 9923534]

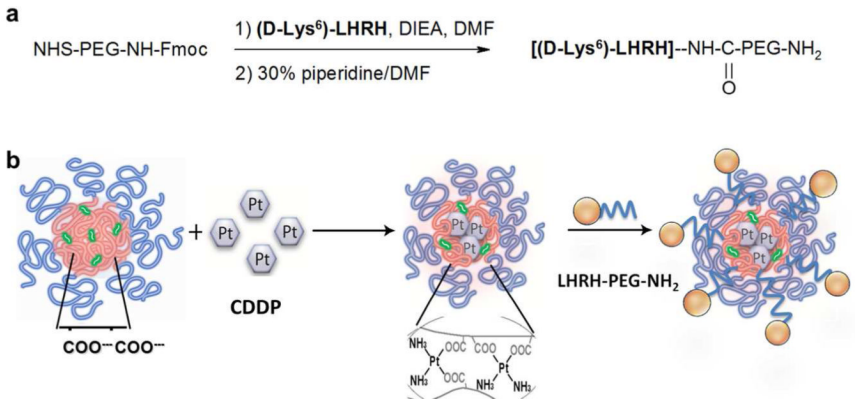

Figure 1.

Scheme for preparation of LHRH-targeted nanogels. **a)** Synthesis of LHRH-PEG-NH_2 and **b)** conjugation of PEGylated LHRH to nanogels. The abbreviations of chemical reagents are summarized in Section 2.2.

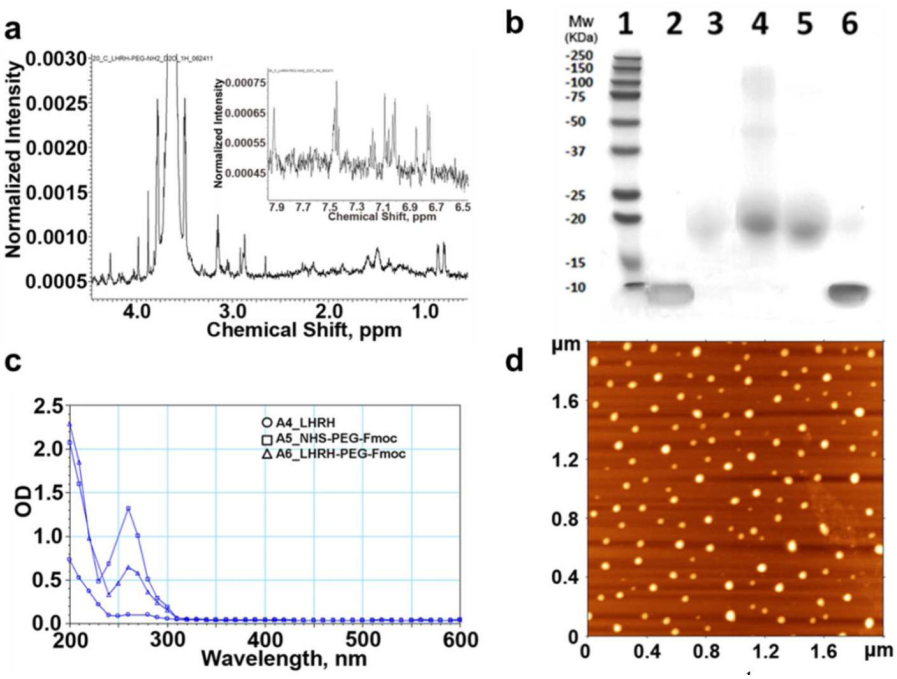

Figure 2.

Characterization of PEGylated peptide and nanogels. **a)** ^{1}H-NMR spectra of the LHRH-PEG-NH_2 in D_2O. **b)** 4-20% Tris-HCl gel followed by Coomassie Blue staining. Lanes: 1. protein ladder, 2. free LHRH, 3. free NHS-PEG-Fmoc, 4. LHRH-PEG modified using 5-fold excess of NHS-PEG-Fmoc, 5. LHRH-PEG synthesized using the equimolar amount of protein and PEG, 6. mixture of LHRH and NHS-PEG-Fmoc. **c)** UV spectra for LHRH and PEGylated LHRH (0.5 mg polymer/ml, PBS). **d)** Tapping-mode AFM images of nanogels deposited from aqueous solutions on the APS-mica. Scan size is 1.8 Zm.

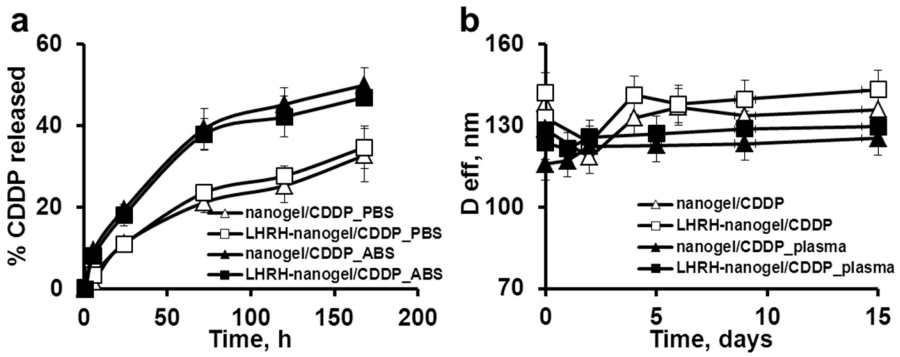

Figure 3.

Drug release and stability of nanogels. **a)** Drug release profiles for CDDP in targeted and untargeted nanogels in PBS, pH 7.4 or ABS, pH 5.5 at 37°C. **b)** Stability of CDDP-loaded untargeted and targeted nanogels in plasma (20% v/v, 37°C) and PBS over time. Data are means ± SD (n = 3).

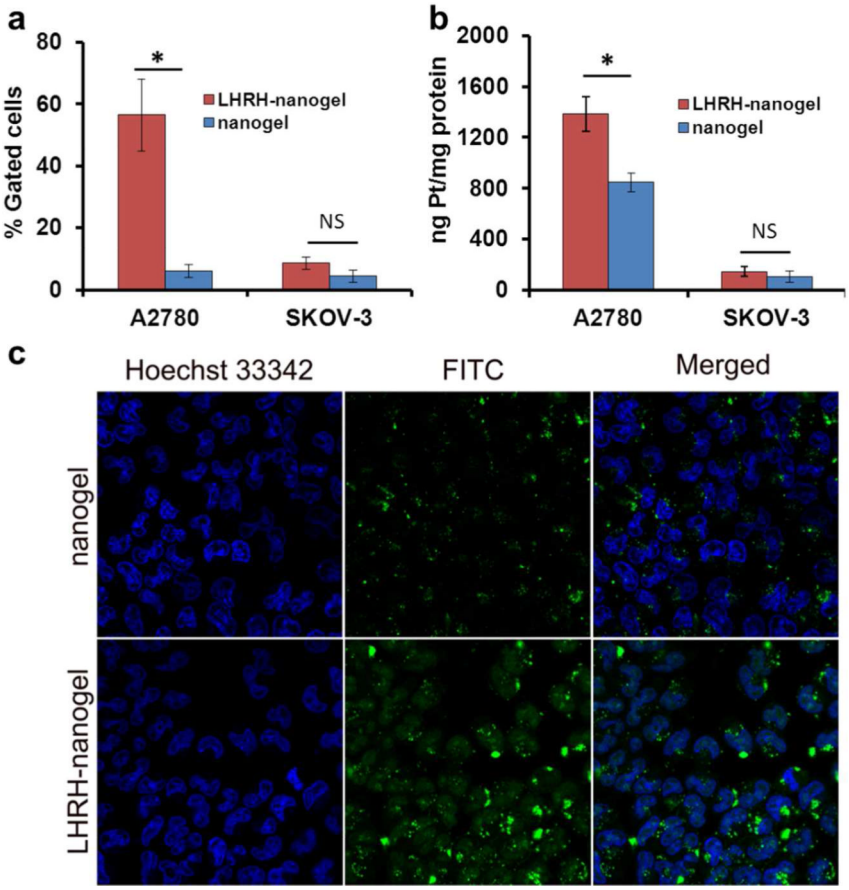

Figure 4.

a) Uptake of FITC-labeled nanogel and LHRH-nanogels by A2780 and SKOV-3 cells (3 h, 37°C, 0.1 mg/ml). **b)** Whole-cell Pt accumulation in A2780 and SKOV-3 cells as measured by ICP-MS (24 h, 37°C, > 0.5 mg/ml). **c)** Confocal micrographs (×63) of nanogel and LHRH-nanogel in A2780 cells. The cells were treated for 3 h with the FITC-labeled nanogels (green), stained with Hoechst 33342 (blue) for nucleus for 10 min at 37°C, followed by live cell imaging. Data are mean ± SD, n = 3, *p < 0.05, NS is not significant.

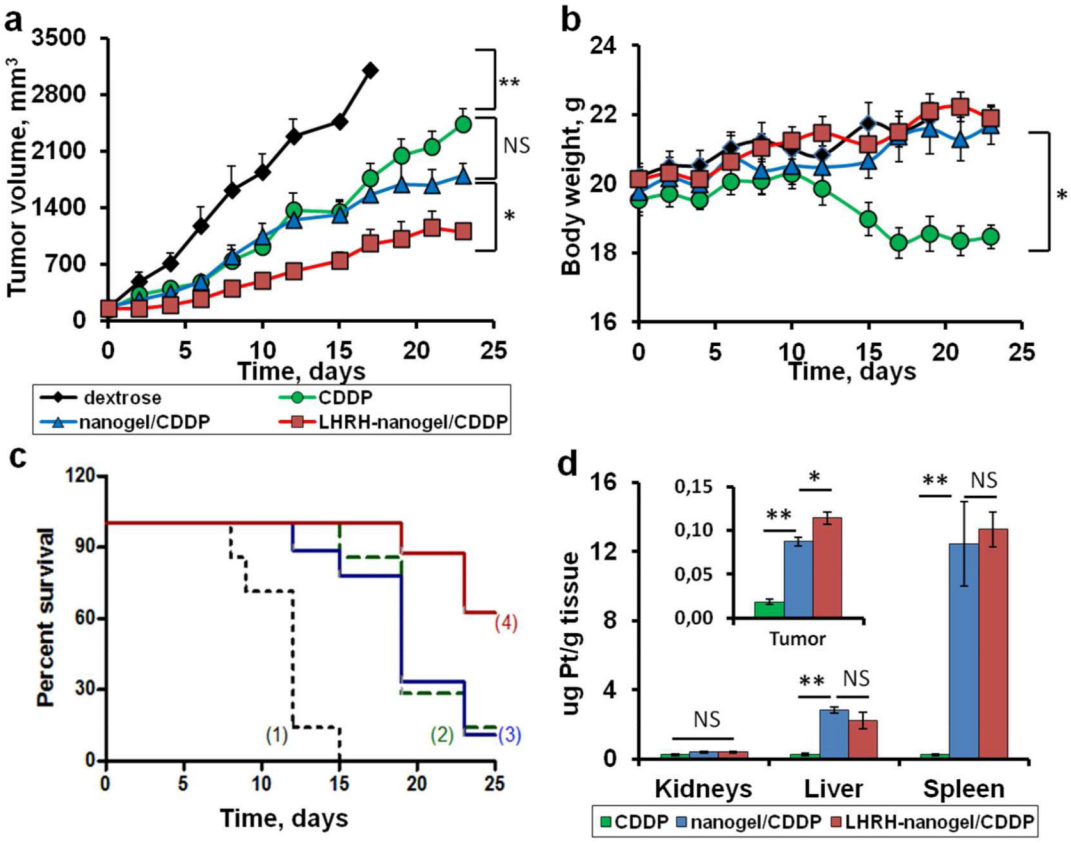

Figure 5.

In vivo antitumor efficacy of CDDP-loaded nanogels and Pt accumulation in A2780 human ovarian cancer xenograft-bearing female nude mice. **a)** Tumor growth, **b)** body weight (calculated as body weight subtract tumor) and **c)** survival time after administration of 5% dextrose (1, control), CDDP alone (2), nanogel/CDDP (3), LHRH-nanogel/CDDP (4) at a dose of 4 mg CDDP equivalents/kg body weight every 4th day. **d)** Concentration of Pt in organs and tumor by ICP-MS. Mice were sacrificed in a week after receiving four *i.v.* injections of free CDDP, nanogel/CDDP and LHRH-nanogel/ CDDP. Data are mean ± SEM, n = 7-8, *p < 0.05, **p < 0.01, NS is not significant.

Table 1

Physicochemical characteristics of nanogels in the absence of elementary salts in water and in PBS. Data are means ± SD (n = 5).

Table 1	DLS						AFM		
	water, pH 7.4			PBS, pH 7.4			PBS, pH 7.4		
Sample	D_{eff}, nm	PdI	ζ-potential, mV	D_{eff}, nm	PdI	ζ-potential, mV	W_{av}, nm	H av, nm	Aspect ratio (W/H)
nanogel	145±3	0.06±0.02	−25.9±0.8	132±4	0.06±0.01	−7.8±1.2	130.9	3.05	43
LHRH-nanogel	139±4	0.09±0.04	−22.1±1.7	128±4	0.07±0.03	−6.8±1.1	136.5	4.49	30

Table 2

Physicochemical characteristics of CDDP-loaded nanogels in the absence of elementary salts in water and in PBS. Data are means ± SD (n = 3).

Table 2	water, pH 7.4			PBS, pH 7.4			
Sample	**D_{eff}, nm**	**PdI**	**ζ-potential, mV**	**D_{eff}, nm**	**PdI**	**ζ-potential, mV**	**LC %**
nanogel/CDDP	132±4	0.08±0.02	−14.7±3	123±5	0.05±0.02	−5.4±0.8	35±3
LHRH-nanogel/CDDP	127±5	0.09±0.01	−14.8±4	119±3	0.07±0.02	−3.2±1.1	38±2